Research Square

Preprints are preliminary reports that have not undergone peer review.
They should not be considered conclusive, used to inform clinical practice,
or referenced by the media as validated information.

Characteristic of anterior Pilon fracture and biomechanical mechanisms: a retrospective study and finite element analysis

Yongwen Dai
The Affiliated Lianyungang Hospital of Xuzhou Medical University
Yu Dong
The Affiliated Lianyungang Hospital of Xuzhou Medical University
Xi Chen
The Affiliated Lianyungang Hospital of Xuzhou Medical University
Kang Song
The Affiliated Lianyungang Hospital of Xuzhou Medical University
Tienan Song
The Affiliated Lianyungang Hospital of Xuzhou Medical University
Deyuan Zhao
The Affiliated Lianyungang Hospital of Xuzhou Medical University
Youhan Mei
The Affiliated Lianyungang Hospital of Xuzhou Medical University
Bo Song
The Affiliated Lianyungang Hospital of Xuzhou Medical University
Gang Xu
760020220019@xzhmu.edu.cn

The First Affiliated Hospital of Kangda College of Nanjing Medical University

Research Article

Keywords: anterior pilon fracture, anterior talofibular ligament, talar cartilage, deltoid ligament, calcaneofibular ligament, post-traumatic osteoarthritis

Posted Date: November 1st, 2026

DOI: https://doi.org/10.21203/rs.3.rs-11268979/v1

License: This work is licensed under a Creative Commons Attribution 4.0 International License.
Read Full License

Additional Declarations: No competing interests reported.

Abstract

Background

Anterior pilon fractures are generally believed to result from axial loading applied to the foot in a dorsiflexed position. However, the patterns of associated periankle injuries and their underlying biomechanical mechanisms remain unclear. This study aimed to characterize the injury associated with anterior pilon fractures and investigate their potential biomechanical mechanisms using finite element analysis.

Methods

A retrospective analysis was performed on the clinical data of 51 patients with anterior pilon fractures who were treated at our institution from March 2018 to August 2026. Clinical data, including medical history, imaging examinations, and surgical records, were collected, and fracture patterns were evaluated to identify the morphological characteristics associated with this injury.Based on these findings, a biomechanical hypothesis regarding the occurrence of anterior pilon fractures was proposed.A finite element model of the ankle joint was established to simulate stress distribution and potential injury sites under different loading conditions.The simulation results were compared with the clinical fracture patterns to validate the proposed injury mechanism.

Results

A total of 51 patients with anterior pilon fractures were included. Among them, talar cartilage (TC) injuries were identified in 18 patients, anterior talofibular ligament (ATFL) injuries in 42 patients, deltoid ligament (DL) injuries in 15 patients, and no calcaneofibular ligament (CFL) injuries were observed.Finite element analysis demonstrated that the Von Mises stress of all evaluated structures generally increased with increasing axial loads from 300 N to 600 N and 1200 N.Among these structures, the stress increases in the DL and ATFL were the most pronounced. The mean stresses of the DL and ATFL increased from 5.52 MPa and 4.39 MPa under a 300 N load to 21.41 MPa and 16.22 MPa under a 600 N load, and further increased to 35.78 MPa and 33.57 MPa under a 1200 N load, respectively.The mean stress of the TC increased from 0.10 MPa at 300 N loading to 4.12 MPa at 600 N and 7.12 MPa at 1200 N.In contrast, the mean stress values of the CFL under the three loading conditions were 1.27, 1.61, and 2.31 MPa, respectively, and remained relatively low throughout.The preoperative VAS score of all patients was 8.2 ± 1.3. No significant pain relief was observed on the first postoperative day, with a VAS score of 7.6 ± 1.5 ($P > 0.05$). However, the VAS scores at 1 month, 3 months, 6 months, 12 months after surgery, and the final follow-up were 2.96 ± 0.90, 1.87 ± 0.44, 0.94 ± 0.38, 0.83 ± 0.44, and 0.87 ± 0.32, respectively. All values showed statistically significant differences compared with the preoperative score ($P < 0.05$), indicating that pain levels significantly decreased compared with preoperative values and gradually stabilized during follow-up.The AOFAS score of all patients increased rapidly from 20.1 ± 8.5

preoperatively to 78.5 ± 7.2 at 1 month after surgery.Subsequently, the score showed a continuous and gradual increase, reaching 95.0 ± 3.1 at 6 months after surgery.At the final follow-up, the AOFAS score remained stable at 94.8 ± 3.5.

Conclusions

Anterior pilon fracture is an intra-articular injury involving the bone–cartilage–ligament complex, and potential occult injuries should be given considerable attention.Ankle arthroscopy facilitates the identification and management of occult injuries.Among these injuries, anterior talofibular ligament (ATFL) injuries and talar cartilage injuries were the most common, followed by deltoid ligament (DL) injuries, while no calcaneofibular ligament (CFL) injuries were observed.Finite element analysis demonstrated significant stress concentration in the anterior talofibular ligament and deltoid ligament, followed by the talar cartilage, whereas the stress in the calcaneofibular ligament remained consistently low.The clinical distribution of injuries and biomechanical analysis collectively suggest that stress transmission, concentration, and local amplification under specific loading conditions may occur during the development of anterior pilon fractures, resulting in the characteristic injury patterns of the ankle joint described above.This study provides a theoretical basis for further understanding the injury mechanism of anterior pilon fractures and optimizing clinical diagnostic and treatment strategies.

Background

Pilon fracture is a unique type of ankle injury involving the distal tibial articular surface, accounting for about 4% -10% of tibial fractures[1, 2]. Anterior pilon fracture is a specific subtype. The classic injury mechanism is considered to involve axial loading of the ankle in dorsiflexion. This force causes a compression or shear fracture of the anterior distal tibia and is often accompanied by varying degrees of articular impaction [3, 4]. Although anterior pilon fracture is inherently an intra-articular injury, its fracture morphology is often relatively simple. Consequently, the overall severity of the injury may be underestimated in clinical practice.

Current clinical evidence suggests that anterior pilon fractures rarely occur as isolated osseous injuries. They are frequently accompanied by talar chondral and ATFL injuries, while DL injury may also occur in some patients. These soft-tissue and intra-articular lesions are often occult. Conventional radiography and CT have limited ability to detect such injuries, and some lesions may remain undiagnosed even when MRI is performed[5–7]. Failure to recognize and treat concomitant chondral injury and residual ligamentous instability may contribute to chronic ankle instability and post-traumatic osteoarthritis (PTOA)[8, 9]. Anterior pilon fractures may be particularly prone to PTOA[10]. Jo et al. reported more severe radiographic PTOA in patients with anterior impaction than in those without it (mean Kellgren–Lawrence grade, 3.1 vs. 2.5). Nishizawa et al. reported PTOA in 39.1% (9/23) of patients with anterior impaction pilon fractures[11–13]. These findings suggest that correction of fracture displacement and

restoration of osseous alignment alone may be insufficient to ensure favorable long-term joint outcomes[11, 13].

In clinical practice, extensive intra-articular injuries may also occur after relatively low-energy trauma. This observation cannot be fully explained by the traditional mechanism of direct axial impact with the ankle in dorsiflexion. It suggests that secondary injury propagation or local stress amplification may occur during the traumatic process. However, several important questions remain unresolved. The distribution of concomitant chondral and ligamentous injuries in anterior pilon fractures has not been systematically characterized. Moreover, the biomechanical mechanisms underlying these occult soft-tissue injuries remain unclear. Consequently, refined and individualized treatment strategies still lack a sufficient mechanistic basis.

Three-dimensional finite element analysis enables quantitative assessment of internal stress distributions under different loading conditions. It can also provide insight into the transmission of mechanical forces within the joint. Therefore, this approach offers a useful biomechanical method for investigating the mechanisms underlying anterior pilon fractures and their associated injuries.

Based on these clinical considerations, the present study combined clinical observations with biomechanical simulation. First, ankle arthroscopy was used to systematically assess concomitant talar chondral and periankle ligamentous injuries and to facilitate their treatment. Second, a detailed three-dimensional finite element model of the ankle was established to evaluate stress distributions under different axial loads. By comparing clinical injury patterns observed during arthroscopy with finite element findings, we aimed to characterize the distribution of associated injuries and explore their potential biomechanical mechanisms. These findings may provide a theoretical basis for more refined, individualized, and arthroscopy-assisted management of anterior pilon fractures.

Methods

Study design and patient population

This study retrospectively analyzed the case information of patients with anterior Pilon fracture admitted to our hospital from March 2018 to August 2026. The inclusion and exclusion criteria are shown in the flowchart (Fig. 1).All patients included at least X-ray, CT or MRI, and ankle arthroscopy was performed in the surgical record and the results were recorded. Because this study is a retrospective data analysis, it does not involve additional interventions for patients, and the study data are anonymized and do not contain personally identifiable information. After the review and approval of the hospital ethics committee, patients can be exempted from the requirement of informed consent.

Data collection

Demographic and clinical variables included age, sex, body mass index (BMI), mechanism of injury, interval from injury to surgery, potential prognostic risk factors, and follow-up status.Mechanisms of injury were categorized as falls from a height of ≤ 3 m, missteps on stairs, motor vehicle accidents, or other/unknown mechanisms. Cases without documented injury mechanisms were included in the latter category.

The interval from injury to surgery was categorized as < 3 days, 3–7 days, and > 7 days. Potential prognostic risk factors included smoking, rheumatoid arthritis, osteoporosis, diabetes mellitus, and hypertension. Follow-up status was categorized as ≥ 12 months, < 12 months, or lost to follow-up (Table 2).

Based on preoperative imaging, all fractures were classified as type 43B according to the AO/OTA classification and type II according to the Rüedi-Allgöwer classification.

Surgical technique

Patients were placed in the supine position under general anesthesia. A tourniquet was applied to the proximal thigh. The operative field was routinely prepared and draped.The standard anteromedial and anterolateral approaches of the ankle joint were established, and the ankle arthroscopy system was placed to explore the tibiotalar joint, talar cartilage, synovial membrane, joint capsule and ankle ligaments.The location, extent, and severity of chondral lesions were assessed arthroscopically. Unstable cartilage margins were debrided. Microfracture was performed for focal cartilage defects when indicated.The tension and continuity of the ATFL and DL were evaluated using an arthroscopic probe. The severity of ligament injury was then determined. Hematoma and interposed soft tissues at the fracture site were removed to facilitate reduction.

After fracture reduction and fixation, ligament stability was reassessed under stress. Ligament repair with sutures was performed when residual instability was identified.

After completion of the intra-articular assessment and treatment, fracture reduction and internal fixation were performed through a limited incision. The posterior articular surface of the distal tibia was used as an anatomical reference for reduction. The fracture fragments were reduced by leverage and temporarily stabilized with Kirschner wires. Bone grafting was selectively performed according to the extent of the osseous defect.Fluoroscopy was used to confirm restoration of the articular surface and satisfactory alignment. Definitive fixation was achieved using a distal tibial T- or L-shaped plate in combination with cannulated screws.After fixation, inversion and eversion stress tests and the Cotton test were performed to assess overall ankle stability. The position of the implant was confirmed by fluoroscopy again, and the incision was irrigated and sutured in layers.

Finite element model construction and loading conditions

CT image acquisition

A healthy 37-year-old male volunteer was selected for model construction. His height was 173 cm and body weight was 60 kg. Radiographic examination confirmed the absence of ankle deformity or osseous abnormalities. He had no history of ankle trauma or surgery.The ankle was scanned using a Siemens 64-detector-row spiral CT scanner. The scanning range extended from the midshaft of the tibia to the plantar surface of the foot. The slice thickness was 0.6 mm, and the pitch was 0.9.Approximately 600 cross-sectional images were obtained and stored in Digital Imaging and Communications in Medicine (DICOM) format. During scanning, the volunteer was positioned supine with the ankle maintained in a neutral position. An immobilization device was used to minimize motion.

Segmentation and three-dimensional reconstruction

The original DICOM images were imported into Mimics 21.0 (Materialise, Belgium) for image segmentation and three-dimensional reconstruction. Bone masks were initially generated using a Hounsfield unit (HU) threshold range of 1121–1776 HU.

The region-growing function was then applied to remove isolated pixels and separate the ankle into individual osseous components. Mask editing and cavity-filling tools were used to refine each bone segment. Redundant regions were manually removed slice by slice, and internal cavities were filled to maintain continuity of the reconstructed contours.

After segmentation of the target bones, ligamentous and cartilaginous structures were reconstructed according to anatomical landmarks and published anatomical data[14, 15]. The reconstructed structures were exported in STL format.

The STL files were imported into Geomagic Wrap 2021 (3D Systems, USA) for surface reconstruction. Mesh defects were identified and repaired, and relaxation and smoothing functions were applied while preserving essential anatomical features. Surface patches were generated and merged into continuous surface models, which were exported in STEP format.

The STEP files were imported into SOLIDWORKS 2023 (Dassault Systèmes, FRA) and assembled into a complete ankle complex by aligning their original coordinate systems. Boolean operations and interference checks were performed, and detected overlaps were corrected. The completed model was then imported into Ansys Workbench 2025 R2 (Ansys, Inc., USA).

Material properties, mesh generation, and loading

All ankle structures were modeled as continuous, isotropic, and linearly elastic materials. Material properties were assigned according to previously published data [16, 17]. The specific parameters are summarized in Table 1. Bones, cartilage, and ligaments were discretized using second-order tetrahedral elements to improve geometric representation of complex anatomical structures. The final model

consisted of approximately 383043 elements and 593839 nodes.To minimize the influence of mesh discretization on the finite element results, a mesh convergence analysis was performed for the established finite element model of the ankle joint. Finite element models with different mesh densities were generated by progressively reducing the mesh size, and numerical simulations were performed under identical conditions. The mesh scheme that satisfied the convergence requirements while maintaining high computational efficiency was selected for subsequent finite element analyses.

A no-separation contact was defined between bone and cartilage. Frictional contact was assigned between opposing cartilage surfaces with a friction coefficient of 0.1. Bone–ligament interfaces were defined as bonded contacts.The ankle was maintained in a neutral position during loading. All degrees of freedom at the plantar weight-bearing surface were constrained. Total axial compressive loads of 300, 600, and 1200 N were applied. The loads were distributed between the tibia and fibula at a ratio of 5:1 [18, 19].Linear static analysis was performed using the static structural solver in Ansys Workbench. Von Mises stress values and spatial distributions in the relevant ankle structures were extracted for further analysis.

Table 1
Summary of model materials and element types

Component	Material type	Young's modulus(MPa)	Poisson's ratio
Bone	Linearly elastic	7300	0.3
Cartilage	Linearly elastic	45	0.42
ATFL	Linearly elastic	255.5	0.4
CFL	Linearly elastic	512	0.4
PTFL	Linearly elastic	216.5	0.4
ATiFL	Linearly elastic	260	0.4
PTiFL	Linearly elastic	260	0.4
TNL	Linearly elastic	320.7	0.4
TSL	Linearly elastic	184.5	0.4
TCL	Linearly elastic	512	0.4
ATTL	Linearly elastic	184.5	0.4
sPTTL	Linearly elastic	99.5	0.4
dPTTL	Linearly elastic	99.5	0.4
Other ligaments	Linearly elastic	260	0.35

Statistical analysis

All statistical analyses were performed using SPSS Statistics version 26.0 (IBM Corp., Armonk, NY, USA). Continuous variables with a normal distribution are presented as the mean ± standard deviation (SD).Comparisons among multiple groups were performed using one-way analysis of variance (ANOVA), followed by the least significant difference (LSD) test for pairwise comparisons. Categorical variables are presented as numbers and percentages.All tests were two-sided, and a P value < 0.05 was considered statistically significant.

Results

Patient characteristics

A total of 51 patients with anterior pilon fractures were included. There were 38 men (74.5%) and 13 women (25.5%). The mean age was 49.86 years (range, 18–72 years), and the mean BMI was 24.90 ± 4.18 kg/m².The mechanisms of injury included falls from a height in 21 patients, falls on stairs in 15, motor vehicle accidents in 13, and other causes in 2. Most patients underwent surgery during the acute phase within 2 weeks after injury.A history of smoking was documented in 36 patients, and 15 had hypertension. None had diabetes mellitus, rheumatoid arthritis, or osteoporosis.Postoperative follow-up was available for 46 patients. Of these, 37 were followed for ≥ 12 months and 9 for < 12 months. Five patients were lost to follow-up(Table 2).

Table 2

Baseline demographic and clinical characteristics of patients with anterior Pilon fractures.

Category	Variables	n(%)
Demographics	Age, years, mean ± SD(range)	49.86 ± 14.96
	Gender	
	Man	38(74.5)
	Fenale	13(25.5)
	BMI, kg/m^2, mean ± SD	24.90 ± 4.18
Mechanism of Injury	Fall fron height(< 3 m)	21(41.2)
	Stair miss/fall	15(29.4)
	Motor vehicle accident	13(25.5)
	Other	2(3.9)
Time from Injury to Surgery, Day	< 3	37(72.5)
	3–7	11(21.6)
	> 7	3(5.9)
Prognostic Factors	Smoking	36(70.6)
	Rheumatoid arthritis	0(0.0)
	Osteoporosis	0(0.0)
	Diabetes	0(0.0)
	Hypertension	15(29.4)
Follow-up, Months	≥ 12	37(72.5)
	< 12	9(17.6)
	Lost	5(9.8)

Injury characteristics of anterior pilon fractures

Integrated assessment of radiographs, CT, MRI, and arthroscopic findings revealed a characteristic pattern of concomitant injuries.ATFL injury(Fig. 2D,I;Fig. 3D,I) was identified in 42 patients (82.4%,Fig. 1). DL injury(Fig. 2F,G,J;Fig. 3F,G,J) was detected in 15 patients (29.4%,Fig. 1) and was predominantly mild to moderate in severity. No CFL injury(Fig. 1;Fig. 2E;Fig. 3E) was observed.Talar chondral injuries(Fig. 2H) were identified in 18 patients (Fig. 1,35.3%)and mainly located in zone 3, with zone 6 also involved in some cases. Zone 3 represented the most frequent site of occult cartilage injury.

Ankle function assessment

VAS and AOFAS scores were scheduled for assessment preoperatively, at postoperative day 1, at 1, 3, 6, and 12 months, and at the final follow-up.

Of the 51 patients initially included, 5 were lost to follow-up and 9 had a follow-up duration of < 12 months. Therefore, 37 patients with ≥ 12 months of follow-up were included in the longitudinal outcome analysis.

VAS scores

The mean preoperative VAS score was 8.21 ± 1.31. At postoperative day 1, the score decreased to 7.60 ± 1.59. The difference from the preoperative value was not statistically significant ($P > 0.05$).

At 1, 3, 6, and 12 months and at the final follow-up, the VAS scores were 2.96 ± 0.90, 1.87 ± 0.44, 0.94 ± 0.38, 0.83 ± 0.44, and 0.87 ± 0.32, respectively. All values were significantly lower than the preoperative score (all $P < 0.05$).

Overall, VAS scores declined progressively after surgery and remained low from 6 months onward (Fig. 4).

AOFAS scores

AOFAS scores increased progressively after surgery (Fig. 5). The mean preoperative score was 18.10 ± 8.45.The scores at postoperative day 1 and at 1, 3, and 6 months were 31.61 ± 5.97, 77.49 ± 6.17, 88.55 ± 4.75, and 93.96 ± 3.30, respectively. At 12 months and the final follow-up, the scores were 93.76 ± 4.11 and 94.02 ± 2.60, respectively.AOFAS scores at all postoperative time points were significantly higher than the preoperative value (all $P < 0.05$). Scores increased substantially during the first 6 months and showed only minor changes thereafter. Values remained above 93 points at 6 months, 12 months, and the final follow-up.

Von Mises stress distributions in the evaluated structures

Finite element analysis was performed under axial loads of 300, 600, and 1200 N. Mechanical responses were assessed in talar cartilage (TC), the fibular attachment site of the ATFL (ATFL-F), the ATFL, the talar attachment site of the ATFL (ATFL-T), the DL, and the CFL.Overall, von Mises stress increased with increasing axial load in all evaluated structures. However, the magnitude of increase varied considerably among structures (Fig. 6).Under the 300 N load, mean stress ranged from 1.27 to 9.16 MPa. The CFL showed the lowest value, whereas the ATFL-F exhibited the highest value.As the load increased, the DL and ATFL showed particularly pronounced increases in stress. Mean DL stress increased from 5.52 MPa at 300 N to 21.41 MPa at 600 N and 35.78 MPa at 1200 N. Corresponding values for the ATFL were 4.39, 16.22, and 33.57 MPa.Under the 1200 N load, the DL showed the highest mean stress at 35.78 MPa. This was followed by the ATFL at 33.57 MPa and ATFL-T at 24.78 MPa. Mean stresses in the TC, ATFL-F, and

CFL were 12.60, 14.38, and 2.31 MPa, respectively.Across all loading conditions, the DL and ATFL demonstrated the greatest increases in stress. In contrast, the CFL consistently exhibited the lowest stress levels.

Discussion

Clinically, it is generally believed that the anterior Pilon fracture is caused by axial violence when the foot is in dorsiflexion[3, 4]. This classic theory is mainly based on the AO/OTA and R Rüedi-Allg Allgöwer classification system with bone structure as the core, which is relatively inadequate for the systematic evaluation of soft tissues other than fractures. With the application of MRI and arthroscopy, clinical workers have gradually realized that Pilon fracture is often accompanied by cartilage and ligament injury, but previous studies have focused on complex Pilon fracture, while there is still a lack of systematic reports on the occurrence and clinical significance of anterior Pilon fracture, a special subtype with low incidence.Our findings indicate that anterior pilon fractures should not be regarded as isolated osseous injuries. Chondral and ligamentous lesions were frequently identified in the present cohort. Arthroscopic examination corroborated many lesions detected on preoperative MRI and also identified additional occult intra-articular abnormalities (Fig. 2H-J; Fig. 3I,J). These findings suggest that a single axial impact to a dorsiflexed ankle may not fully explain the entire spectrum of injury. Instead, anterior pilon fractures may involve a more complex interaction among the osseous, chondral, and ligamentous components of the ankle.

The clinical injury pattern observed in this study suggests that the anterior Pilon fracture may be a continuous injury. A significant proportion of patients are injured after falling on stairs or from a relatively limited height. However, it eventually leads to articular surface compression, talus cartilage injury and ligament injury. These findings can hardly be fully attributed to the magnitude of the initial external force. Based on the comprehensive clinical and biomechanical observations, we believe that the initial violence may be the initiating factor of the injury. During axial loading in ankle dorsiflexion, the tibiotalar contact moves forward, reducing the effective contact area and increasing the local contact stress[20]. When the anterior articular surface of the distal tibia is destroyed, subluxation or transient dislocation of the talus occurs. The anterior talofibular ligament is most susceptible to rupture because it is relatively weak and is the main structure that limits the anterior movement of the talus[21]. Loss of ATFL constraint may further alter the position of the talus in the ankle mortise and redistribute stress over the remaining stable structure[18]. During this process, secondary impingement may occur between the talar roof and the injured tibial articular surface. Such an event may further damage the cartilage already damaged in the initial impact. Such acute cartilage injury may initiate biological and mechanical pathways that contribute to progressive joint degeneration and the subsequent development of PTOA[22, 23]. Our findings therefore provide biomechanical support for the possibility of transient anterior talar subluxation during the injury process[24].This may also explain why the extent of intra-articular damage is sometimes out of proportion to the apparent energy of the initial trauma. However, this sequential mechanism is still a hypothesis and needs to be confirmed by dynamic biomechanical and experimental studies.

The present finite element analysis demonstrated increased stress in TC as the axial load increased. Stress concentration was particularly evident in zone 3. This finding was consistent with the arthroscopic observations. TC lesions involving zone 3 and/or zone 6 were identified in 18 patients (35.3%) (Fig. 2H). Experimental studies using porcine models of pilon fractures have demonstrated that chondrocyte death is spatially associated with the site of injury, with greater cell death occurring near the fracture margin and following higher-energy impacts[22]. This spatial relationship is consistent with our observations.Our study further demonstrated a high incidence of associated ligament injuries in patients with anterior pilon fractures. ATFL lesions were identified in 42 patients (82.4%), whereas DL lesions were observed in 15 patients (29.4%). These clinical findings were consistent with the finite element analysis, which showed significantly increased stress in both the ATFL and DL (Fig. 6). However, the incidence of DL injury was considerably lower than that of ATFL injury in clinical observations, which was not completely consistent with the stress distribution observed in the finite element analysis. This discrepancy may be explained by the following factors:First, The ATFL and DL differ substantially in their geometry and mechanical properties. The ATFL is a relatively thin structure and has been shown to exhibit a lower load to failure, whereas major components of the deep deltoid ligament possess substantially greater mechanical strength[25, 26]. These intrinsic differences may partly explain why a high stress magnitude does not necessarily translate into the same risk of structural failure across different ligaments.Second, The DL is a broad, fan-shaped complex composed of multiple bundles with distinct orientations and functions. This architecture may facilitate load sharing among bundles under different ankle positions and loading conditions, thereby reducing stress concentration within any single component[27]. Third, the loading conditions used in the present model were necessarily idealized. Actual ankle trauma is a dynamic and multiplanar process involving complex combinations of translational and rotational forces. In addition to dorsiflexion and axial compression, inversion, eversion, internal or external rotation, and variations in the magnitude and rate of loading may substantially alter the mechanical response of individual ankle ligaments[16]. Fourth, the injury process may be dynamic and sequential rather than static. High-energy axial loading during dorsiflexion may result in compression or destruction of the anterior lip of the tibia, secondary anterior displacement or subluxation of the talus[3]. This displacement may increase the tension load of the ATFL[21]. Brady et al showed that a major biomechanical role of the DL is to resist eversion and external rotation[28]. This mechanism may partly explain the higher prevalence of ATFL than DL lesions in our cohort, although further dynamic validation is needed. Thus, the finite element model represents stress at a defined loading state, whereas clinical ligament rupture reflects the cumulative effects of load magnitude, direction, loading rate, duration, tissue strength, and the sequence of structural failure.The discrepancy between simulated stress and observed ligament injury therefore does not necessarily represent a contradiction. Rather, it highlights the limitation of predicting ligament rupture solely from von Mises stress. It also emphasizes the need to interpret finite element findings together with arthroscopic and clinical observations.

Post-traumatic osteoarthritis (PTOA) is a common complication following intra-articular ankle fractures. Wang et al. retrospectively evaluated 477 patients who underwent open reduction and internal fixation

for ankle fractures and reported radiographic PTOA in 34.2% of patients at a mean follow-up of 4.3 years[29]. Notably, anterior pilon fractures appear to be associated with particularly unfavorable joint outcomes. In a comparative cohort study, Jo et al. found that patients with anterior impaction had significantly more advanced radiographic PTOA than those without anterior impaction, as well as a higher rate of implant removal for pain (39% vs. 13%)[13]. These findings highlight the substantial risk of post-traumatic joint degeneration and persistent symptoms associated with anterior pilon fractures.Disruption of the lateral or medial ankle ligaments may compromise tibiotalar stability and result in abnormal talar motion[18, 30]. Repeated abnormal loading after injury may further promote cartilage degeneration and contribute to the development of PTOA[11].These observations reinforce the importance of evaluating the ankle as an integrated joint rather than focusing exclusively on fracture reduction. Arthroscopy may be particularly useful for identifying chondral lesions and ligament abnormalities that are not readily apparent on routine imaging. Previous experimental work has also suggested that irreversible chondrocyte injury may occur despite an apparently intact cartilage surface[22]. Restoration of the articular surface alone may therefore not fully address the biological and mechanical consequences of anterior pilon fractures.Therefore, clinical treatment requires not only the restoration of bony anatomy. Careful evaluation of ligament integrity and articular cartilage is also necessary. Associated lesions should be treated when clinically indicated. Arthroscopy provides direct visualization of these structures and can be used as a complement to preoperative imaging. Recognition of complete injury patterns may also improve patient counseling, prognostic assessment, and postoperative rehabilitation planning. Whether adjuvant arthroscopic treatment and concomitant management of associated lesions can reduce the long-term incidence of PTOA requires further investigation.

Limitations

This study has several limitations. First, anterior pilon fractures are relatively uncommon, and the clinical sample was limited. The follow-up period was also insufficient to fully determine the long-term relationship between TC injury and PTOA. In addition, no control group was included. Therefore, the incremental clinical benefit of ligament repair or chondral treatment could not be established. Second, VAS and AOFAS scores were used as the principal clinical outcome measures. These assessments may be influenced by patient-related factors and contain subjective components. Future studies should incorporate additional quantitative assessments, including gait analysis and other validated functional outcome measures. Third, the finite element model was constructed from CT data obtained from a single healthy volunteer. Bones, cartilage, and ligaments were modeled using simplified homogeneous, isotropic, and linearly elastic material assumptions. Static loading was applied, whereas actual traumatic events are dynamic and involve complex interactions among impact velocity, multiplanar motion, muscle activation, and time-dependent tissue behavior. These simplifications may partly explain the discrepancy between predicted DL stress and the lower incidence of DL injury observed clinically.Moreover, the current model evaluated stress distribution rather than tissue-specific failure thresholds. It therefore cannot directly predict ligament rupture. Future studies should incorporate cadaveric experiments,

dynamic impact testing, and more physiologically realistic material properties to improve model validation. Larger prospective cohorts and longer follow-up are also needed to clarify the progression of cartilage injury and the long-term development of ankle degeneration.

Conclusions

Anterior pilon fracture is an intra-articular injury involving the bone–cartilage–ligament complex, and potential occult injuries should be given considerable attention.Ankle arthroscopy facilitates the identification and management of occult injuries.Among these injuries, ATFL and TC injuries were the most common, followed by DL injuries, while no CFL injuries were observed.Finite element analysis demonstrated significant stress concentration in the ATFL and DL, followed by the TC, whereas the stress in the CFL remained consistently low.The clinical distribution of injuries and biomechanical analysis collectively suggest that stress transmission, concentration, and local amplification under specific loading conditions may occur during the development of anterior pilon fractures, resulting in the characteristic injury patterns of the ankle joint described above.This study provides a theoretical basis for further understanding the injury mechanism of anterior pilon fractures and optimizing clinical diagnostic and treatment strategies.

Abbreviations

AOFAS
American Orthopaedic Foot & Ankle Society
ATFL
Anterior talofibular ligament
ATFL-F
Fibular attachment site of the anterior talofibular ligament
ATFL-T
Talar attachment site of the anterior talofibular ligament
BMI
Body mass index
CFL
Calcaneofibular ligament
CT
Computed tomography
DL
Deltoid ligament
MRI
Magnetic resonance imaging
PTOA
Post-traumatic osteoarthritis
TC

Talar cartilage
VAS
Visual analog scale

Declarations

Ethics approval and consent to participate

This retrospective study was conducted according to the principles of the Declaration of Helsinki and approved by the Academic Committee of Lianyungang First People's Hospital(Approval No. KY-20261007004-01). And was granted an exemption from informed consent. The specific reasons for the exemption are detailed in the application documents for the exemption of informed consent.

Clinical trial number

Not applicable.

Consent for publication

Not applicable.

Availability of data and materials

The datasets used and/or analysed during the current study are available from the corresponding author on reasonable request.

Competing interests

The authors declare that they have no competing interests.

Funding

This study was supported by the Clinical Research Fund of the First People’s Hospital of Lianyungang (Grant No. LC23).

Authors' contributions

Yongwen Dai contributed to the interpretation of the results and drafted the original manuscript. Yu Dong performed three-dimensional reconstruction, finite element model construction, loading and boundary condition settings, and finite element analysis. Xi Chen, Kang Song and Deyuan Zhao were responsible for clinical data collection and preparation of CT data. Tienan Song and Bo Song were responsible for clinical case diagnosis and assessment. Youhan Mei performed data analysis and contributed to the interpretation of the results. Gang Xu conceived and designed the study, supervised the research, and provided methodological guidance. Yongwen Dai and Yu Dong contributed equally to this work and share co-first authorship. All authors reviewed and approved the final manuscript.

Acknowledgements

The authors would like to thank Dr. Xiaoshuang Xu for her valuable guidance and advice on the statistical methodology used in this study.

AI-Assisted Language Editing

During the preparation of this manuscript, the authors used ChatGPT (OpenAI) solely to improve the language, grammar, and readability of the manuscript. The tool was not used to generate or analyze research data, interpret the results, or formulate scientific conclusions. All AI-assisted revisions were carefully reviewed and edited by the authors, who take full responsibility for the final content of the manuscript.

References

1. Gao Y, Zhu H, Guo Y, Yu X. Early Reduction of the Posterior Column: A Surgical Technique in AO/OTA C3 Tibial Pilon Fractures. J Pers Med. 2023;13(3). 10.3390/jpm13030551.
2. Liu J, Piao C, Cui G, Sun H, Li Z. Fracture Line Morphology and a Novel Classification of Pilon Fractures. Orthop Surg. 2025;17(2):540–50. 10.1111/os.14304.
3. Nishizawa G, Futamura K, Izawa Y, Nishida M, Inagaki N, Saito M. Reconstruction strategy and outcomes for anterior impaction pilon fractures. Int Orthop. 2026;50(8):1889–98. 10.1007/s00264-026-06828-w.
4. Gulbrandsen TR, Wynn M, Garrone AJ, Hulick RM, Spitler CA, Crist BD. Does Anterior Impaction Affect Radiographic Outcomes of Pilon Fractures? Iowa Orthop J. 2022;42(2):30–5.
5. Zhang D, Zhong X, Zhang S. Outcome analysis of modified lateral malleolar osteotomy for the management of talar body fractures associated with tibial pilon fractures. Front Surg. 2026;13:1843849. 10.3389/fsurg.2026.1843849.
6. Darwich A, Nörenberg D, Adam J, Hetjens S, Bdeir M, Schilder A, et al. Higher Accuracy of Arthroscopy Compared to MRI in the Diagnosis of Chondral Lesions in Acute Ankle Fractures: A Prospective Study. Diagnostics (Basel). 2024;14(16). 10.3390/diagnostics14161810.
7. Darwich A, Nörenberg D, Adam J, Hetjens S, Schilder A, Obertacke U, et al. A Multi-Disciplinary MRI Assessment May Optimize the Evaluation of Chondral Lesions in Acute Ankle Fractures: A Prospective Study. Diagnostics (Basel). 2023;13(20). 10.3390/diagnostics13203220.
8. Hong CC, Tan KJ, Calder J. Chronic lateral ankle ligament instability - Current evidence and recent management advances. J Clin Orthop Trauma. 2024;48:102328. 10.1016/j.jcot.2023.102328.
9. Wijnhoud EJ, Rikken QGH, Dahmen J, Sierevelt IN, Stufkens SAS, Kerkhoffs G. One in Three Patients With Chronic Lateral Ankle Instability Has a Cartilage Lesion. Am J Sports Med. 2023;51(7):1943–51. 10.1177/03635465221084365.
10. Li X, Xu Y, Guo C, Yang C, Zhu Y, Xu X. Anterior distal tibial plafond-plasty for the treatment of posttraumatic ankle osteoarthritis with anterior translation of the talus. Sci Rep. 2021;11(1):4381.

10.1038/s41598-021-83946-y.

11. Anderson DD, Ledoux WR, Lenz AL, Wilken J, Easley ME, de Cesar Netto C. Ankle osteoarthritis: Toward new understanding and opportunities for prevention and intervention. J Orthop Res. 2024;42(12):2613–22. 10.1002/jor.25973.
12. Chalidapong P, Vaseenon T, Chattipakorn N, Chattipakorn SC. Potential Roles of Inflammation on Post-Traumatic Osteoarthritis of the Ankle. Int J Mol Sci. 2024;25(11). 10.3390/ijms25115903.
13. Jo S, Tilan J, McAndrew C, Miller AN. Poor Outcomes After Anterior Impaction Pilon Fractures. J Am Acad Orthop Surg. 2022;30(1):19–26. 10.5435/jaaos-d-20-01329.
14. Dalmau-Pastor M, Malagelada F, Guelfi M, Kerkhoffs G, Karlsson J, Calder J, et al. The deltoid ligament is constantly formed by four fascicles reaching the navicular, spring ligament complex, calcaneus and talus. Knee Surg Sports Traumatol Arthrosc. 2024;32(12):3065–75. 10.1002/ksa.12173.
15. Fujishiro H, Nimura A, Azumaya M, Hattori S, Hoshi O, Akita K. Anatomical study of the bone morphology of the anterior talofibular ligament attachment. Anat Cell Biol. 2023;56(3):334–41. 10.5115/acb.23.002.
16. Li Y, Yang Q, Zhang Q, Wang H, Cheng CK. Investigation of acute and chronic injury mechanisms of the deltoid ligament: insights from finite element analysis and animal study. J Orthop Surg Res. 2026;21(1). 10.1186/s13018-026-06860-x.
17. Li Y, Tong J, Wang H, Ji X, Hua Y, Cheng CK. Investigation into the effect of deltoid ligament injury on rotational ankle instability using a three-dimensional ankle finite element model. Front Bioeng Biotechnol. 2024;12:1386401. 10.3389/fbioe.2024.1386401.
18. Ji S, Sun L, Wang Q, Qi H, Wu B, Du B, et al. The impact of lateral ankle ligament injuries on ankle stability and talar cartilage stress: a finite element analysis of combined injury mechanisms. Front Bioeng Biotechnol. 2025;13:1697096. 10.3389/fbioe.2025.1697096.
19. Lan X, Mo J, Gao J, Li Y, Kang G, He D, et al. Effects of graded talar external rotation on distal tibial articular surface stress and contact pressure: a finite element study. Front Sports Act Living. 2026;8:1810571. 10.3389/fspor.2026.1810571.
20. Peiffer M, Lewis L, Xie K, Guild TT, Ashkani-Esfahani S, Kwon J. The Influence of Talar Displacement on Articular Contact Mechanics: A 3D Finite Element Analysis Study Using Weightbearing Computed Tomography. Foot Ankle Int. 2024;45(4):393–405. 10.1177/10711007241227179.
21. Dalmau-Pastor M, El-Daou H, Stephen JM, Vega J, Malagelada F, Calder J. Clinical Relevance and Function of Anterior Talofibular Ligament Superior and Inferior Fascicles: A Robotic Study. Am J Sports Med. 2023;51(8):2169–75. 10.1177/03635465231172196.
22. DeKeyser GJ, Thorne TJ, Olsen A, Haller JM. Porcine Pilon Fractures Result in Significant Chondrocyte Cell Death on Both Sides of the Tibiotalar Joint. Foot Ankle Int. 2025;46(8):827–35. 10.1177/10711007251341310.
23. Dilley JE, Bello MA, Roman N, McKinley T, Sankar U. Post-traumatic osteoarthritis: A review of pathogenic mechanisms and novel targets for mitigation. Bone Rep. 2023;18:101658.

10.1016/j.bonr.2023.101658.

24. McKinley TO, Tochigi Y, Rudert MJ, Brown TD. Instability-associated changes in contact stress and contact stress rates near a step-off incongruity. J Bone Joint Surg Am. 2008;90(2):375–83. 10.2106/jbjs.G.00127.
25. Shao Q, Hu D, Chen X, Wang H, Xiao L, Teng Q, et al. Comparison of Suture Anchor Repair and Suture Tape Augmentation for Reconstruction of the Anterior Talofibular Ligament: A Biomechanical Study. Orthop Surg. 2025;17(1):244–51. 10.1111/os.14284.
26. Inchai C, Vaseenon T, Tanaka Y, Mahakkanukrauh P. The Specific Anatomical Morphology of Lateral Ankle Ligament: Qualitative and Quantitative Cadaveric based Study. Orthop Surg. 2023;15(10):2683–8. 10.1111/os.13872.
27. Mori Y, Murahashi Y, Takahashi K, Horita K, Kamiya T, Emori M, et al. Load sharing and stability of deltoid ligament during ankle motion loading-A cadaveric biomechanical study. Clin Biomech (Bristol). 2026;137:106875. 10.1016/j.clinbiomech.2026.106875.
28. Takahashi K, Teramoto A, Murahashi Y, Shiwaku K, Kamiya T, Emori M, et al. The In Situ Force and Contribution of Each Ligamentous Band of the Deltoid Ligament in Ankle Joint Stability: A Cadaveric Biomechanical Study. Orthop J Sports Med. 2025;13(4):23259671251327406. 10.1177/23259671251327406.
29. Wang L, Ji C, Zhang X, Wang L, Liu T, Sun H, et al. Post-traumatic osteoarthritis after ankle fracture fixation: A minimum three-year follow-up. Foot Ankle Surg. 2025;31(7):576–82. 10.1016/j.fas.2025.02.014.
30. Li Y, Ji X, Yang Q, Wang H, Cheng CK. The Role of the Individual Bundles of the Deltoid Ligament in Multidirectional Stability and Articular Contact Pressure of the Ankle Joint: A Finite Element Analysis. Bioeng (Basel). 2026;13(2). 10.3390/bioengineering13020145.

Figures

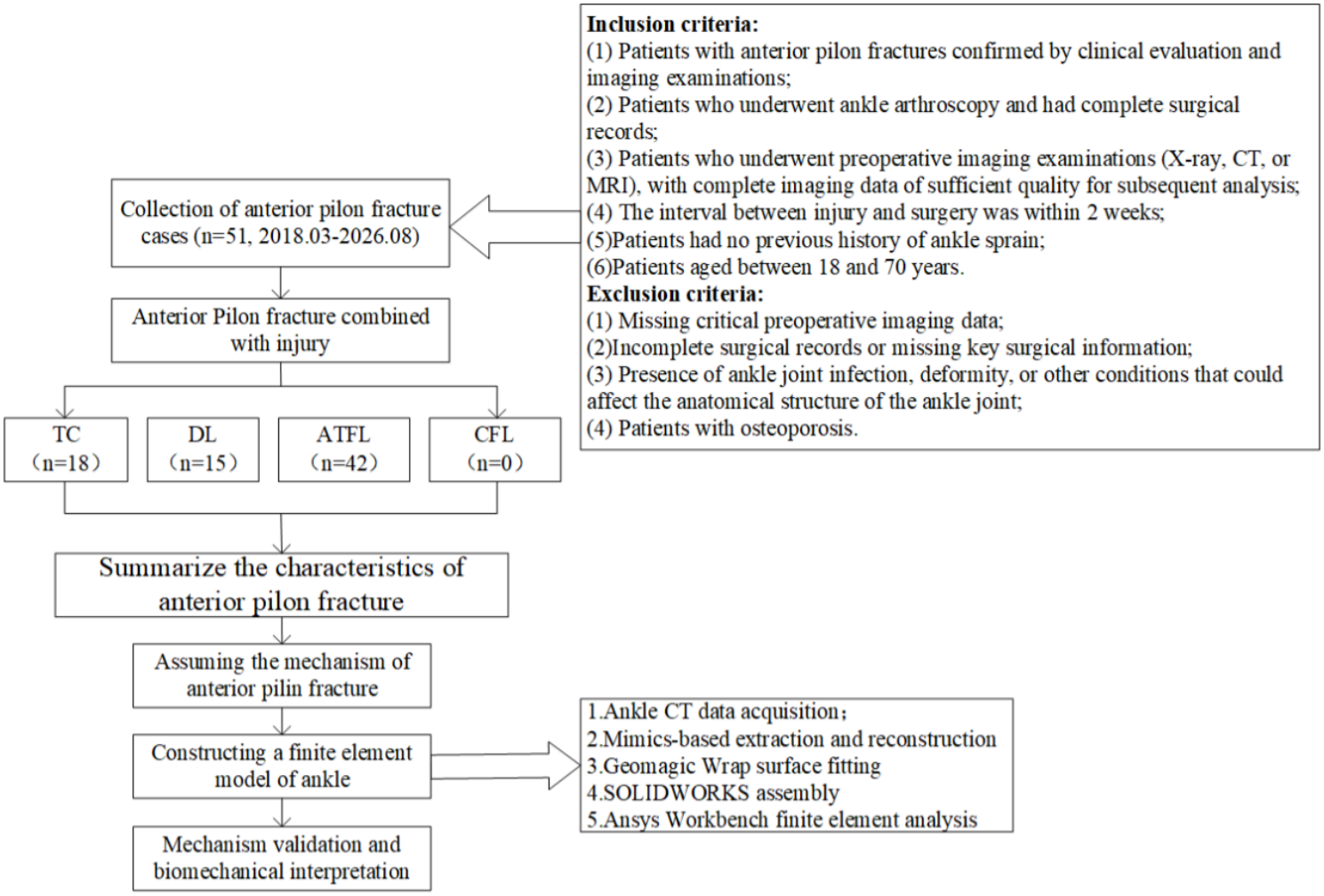


Figure 1

Flowchart

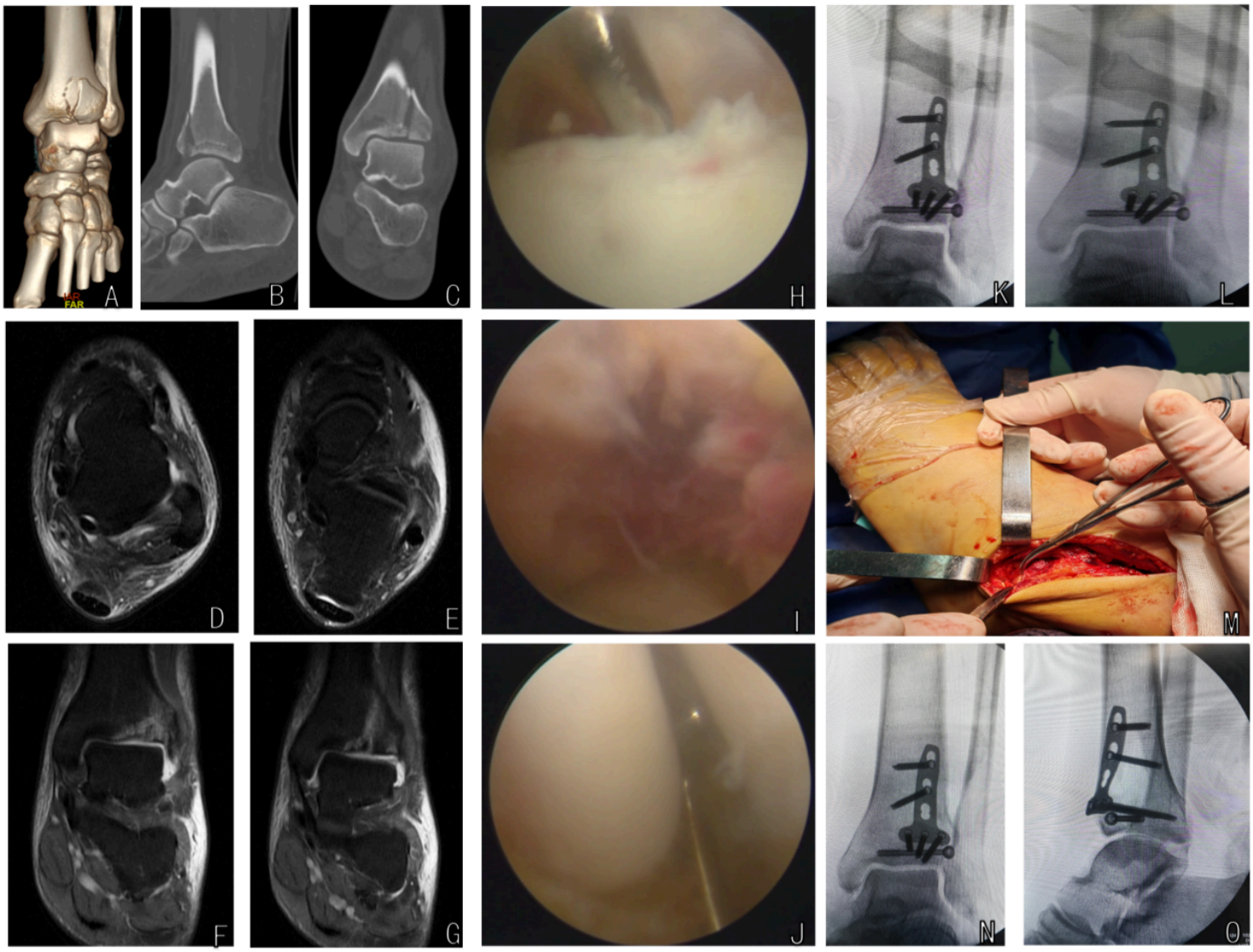


Figure 2

A young and middle-aged man was admitted to the hospital because of "falling down to the left ankle swelling and pain with limited movement for 8 days". A-G: preoperative CT and MR, indicating fracture of left tibial anterior edge, injury of talus cartilage, injury of anterior talofibular ligament (grade III), and injury of triangular ligament (grade I); H-J: injury of talus cartilage (zone 3), rupture of anterior talofibular ligament, and injury of triangular ligament under arthroscopy; K: positive ankle stress test; L: Ankle joint stress test was negative (after ligament repair); M: Anterior talofibular ligament was ruptured and repaired; N-O: Anteroposterior and lateral ankle joint after operation.

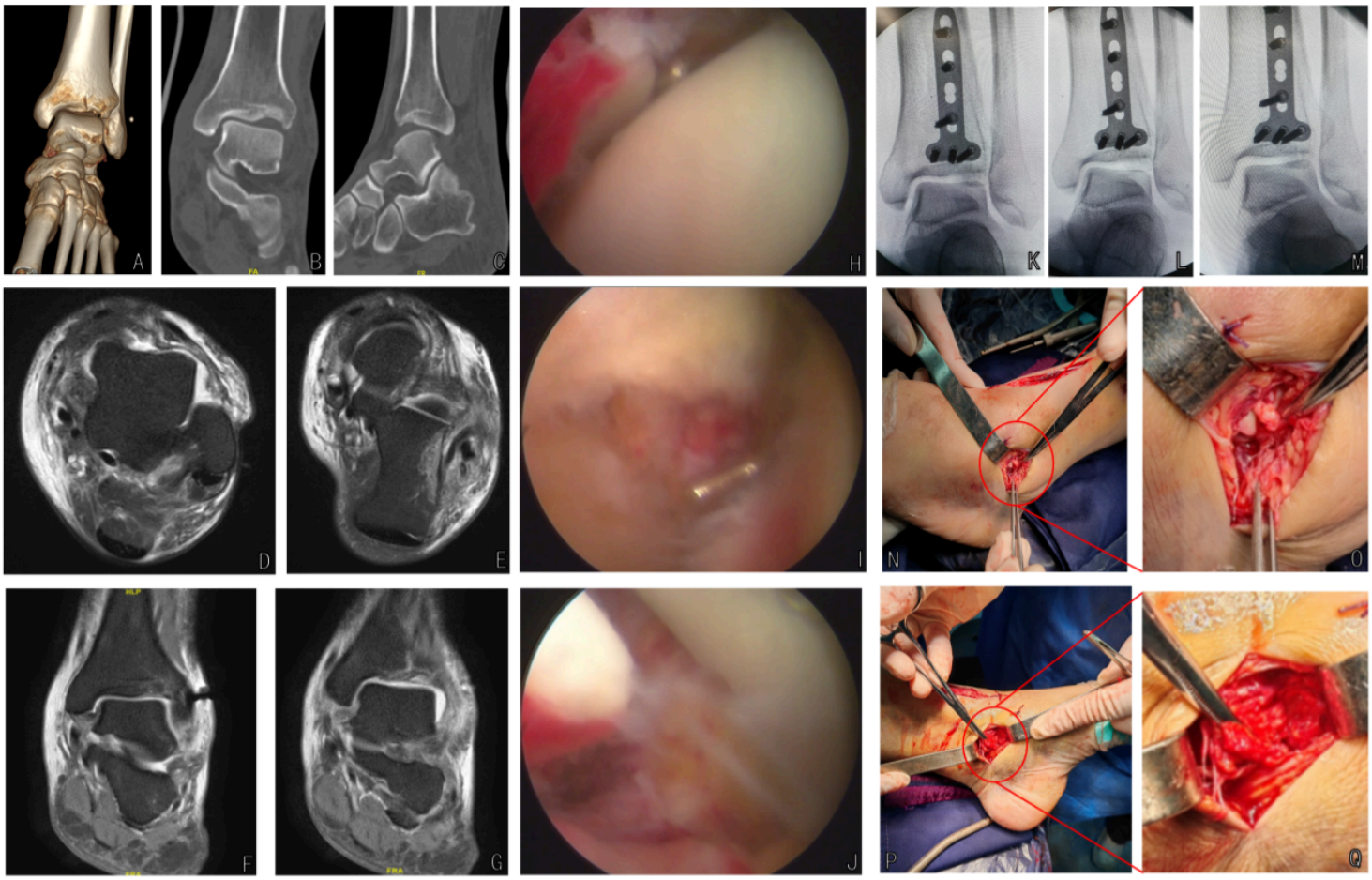


Figure 3

A middle-aged man was admitted to the hospital because of "left ankle swelling, pain and limitation of movement for 2 days caused by falling from a height of 2 meters". A-G: preoperative CT and MR showed left tibial anterior fracture, anterior talofibular ligament injury (Grade III) and deltoid ligament injury (Grade II); H-J: intraoperative arthroscopy showed no injury of talus cartilage, rupture of anterior talofibular ligament and rupture of deltoid ligament; K: no obvious abnormality of static ankle acupoint after internal fixation; L-M: positive ankle stress test; N, O: rupture of anterior talofibular ligament; P, Q: tear of deltoid ligament.

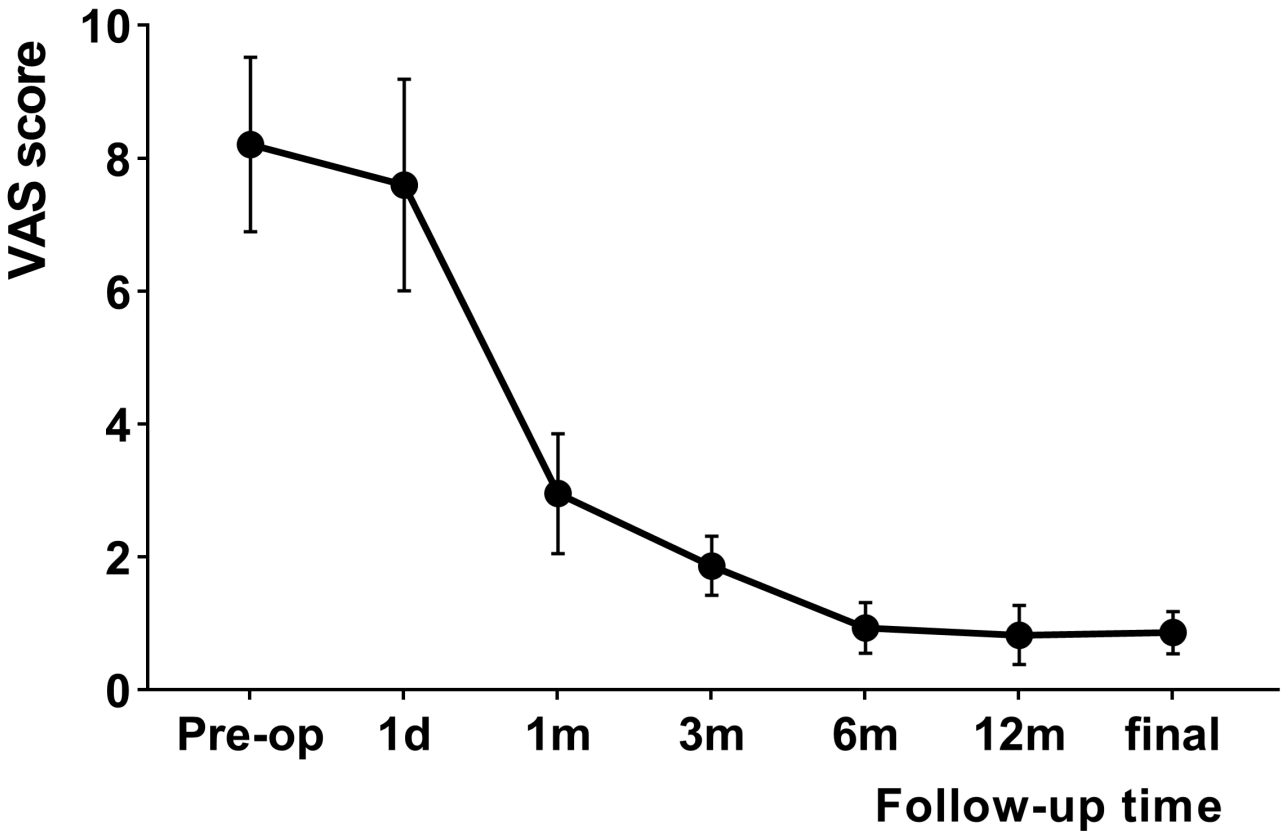


Figure 4

Graphs of VAS Scores over Time

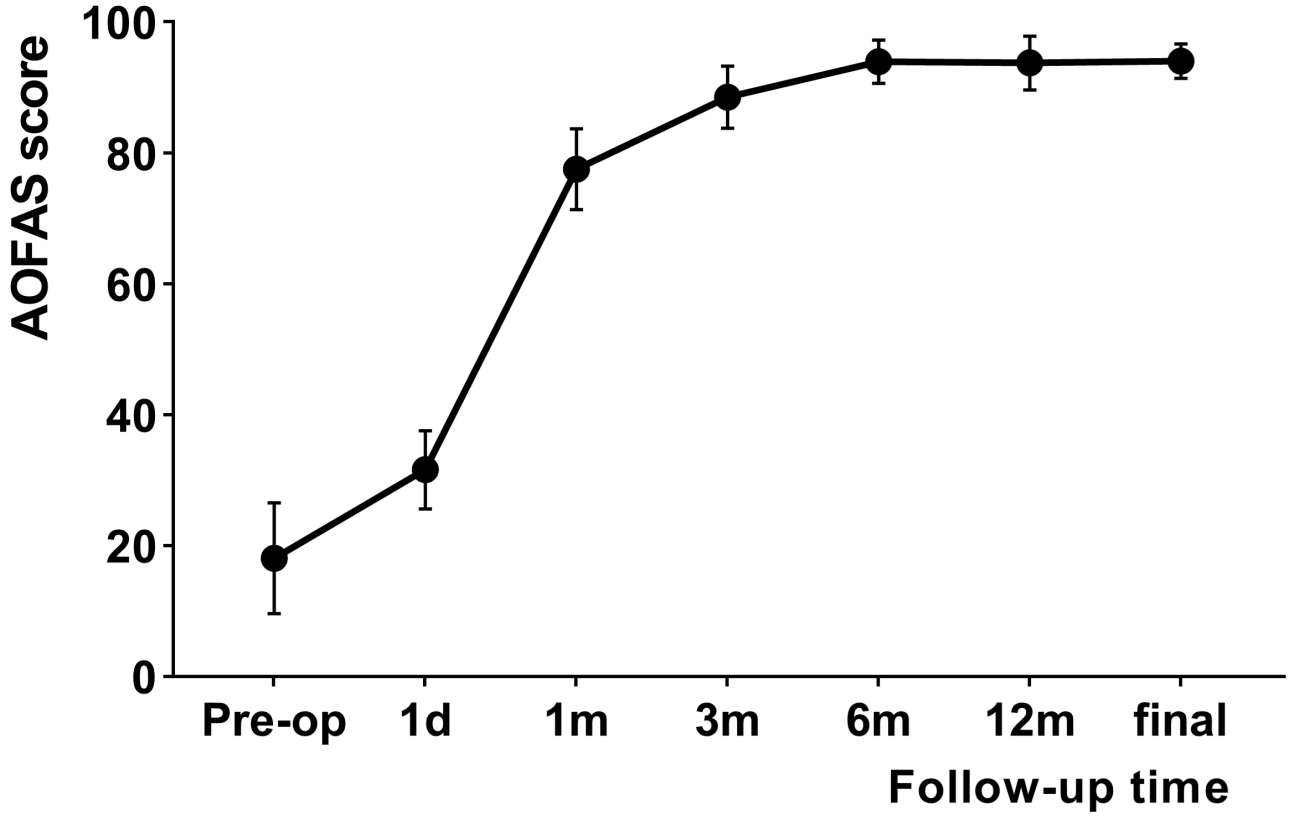


Figure 5

Graphs of AOFAS Scores over Time

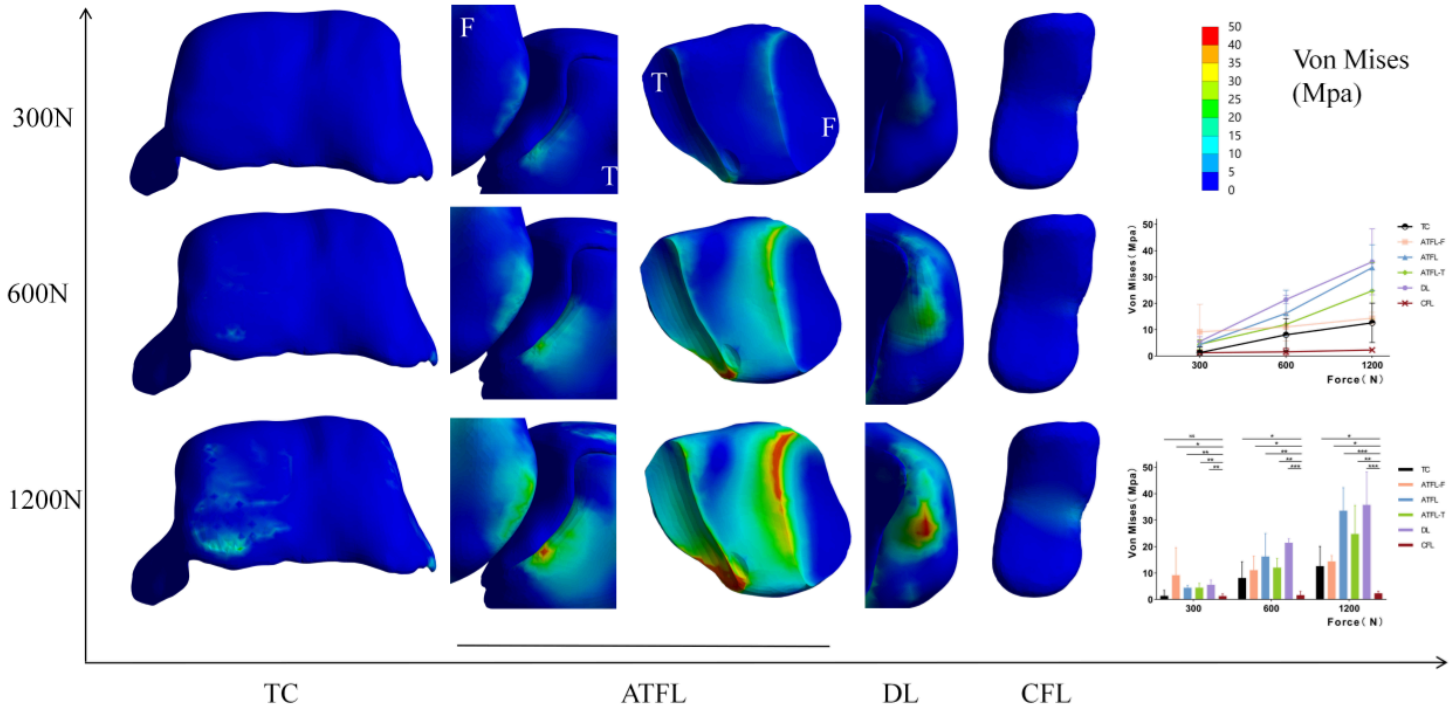


Figure 6

Von Mises stress distribution of TC, ATFL, DL and CFL